

Single sheet tester for measuring core losses with novel adaptive algorithm of waveform

TOMASZ LERCH[✉], MICHAŁ RAD[✉], WITOLD RAMS

*Faculty of Electrical Engineering, Automatics, Computer Science, and Biomedical Engineering
AGH University of Science and Technology
al. Mickiewicza 30, 30-059 Krakow, Poland
e-mail: lerch/rad/rams@agh.edu.pl*

(Received: 23.03.2022, revised: 10.06.2022)

Abstract: This paper presents a novel method of waveform generation in a single-sheet tester (SST) for measuring core losses and permeability in a steel sheet. Some improvements and modifications of the apparatus are also described. The improved way of working of a SST is important, especially in the extended range of polarization (up to 1.9 T). The system consists of hardware and software. Everything together was tested and has given good results. The proposed algorithm is described and compared to previously known methods.

Key words: core losses, efficiency, Epstein, hysteresis, magnetization

1. Introduction

The new standard IEC 60034–30 (International Electrotechnical Commission), published in 2011, introduces the method of assessing the efficiency ranges of all motors launched to the European market. In light of the current standard, the class IE2 is required. The efficiency achieved by electrical machines depends on winding losses, magnet core losses and mechanical losses. Of the above-mentioned, the most difficult to quantify in the design stage are the core losses. This is due to, inter alia, not very precise methods of measuring sheet losses from which the cores are made. Therefore, the proper measurement of magnetic characteristics and core losses is still a vital problem in the construction of electrical machines. Not only are the parameters of the original iron sheets important, but determination of such impact factors such as stress, distortion, temperature, production procedure – is very often needed [1–3]. In such cases, the Epstein frame is not valid. The single-sheet test (SST) method is more involved. However, the SST method is not ideal and is still under investigation by scientists [4, 5]. There are two main problems:



© 2022. The Author(s). This is an open-access article distributed under the terms of the Creative Commons Attribution-NonCommercial-NoDerivatives License (CC BY-NC-ND 4.0, <https://creativecommons.org/licenses/by-nc-nd/4.0/>), which permits use, distribution, and reproduction in any medium, provided that the Article is properly cited, the use is non-commercial, and no modifications or adaptations are made.

getting a properly distributed field in a specimen and to obtain sinusoidal waveform of dB/dt (output voltage). An additional difficulty in determining the losses by the SST apparatus is the correct measurement of the field strength. A number of works have been devoted to this problem. The article [6] describes the use of KMZ10B magnetoresistive sensors, which have dimensions smaller than those used in the described structure, but the measurement range is not sufficient in relation to the assumed one. In [7] it was shown that when using the excitation coil of the design according to the Standards, there is a strong variation in the H value along with the distance from the sheet surface. The H -field sensor must therefore be very close to the plate. For these reasons, it was decided to excite the field with a system of two coils, analogous to the Helmholtz system. They do not enclose tightly tested sample, thus creating a sufficient area to accommodate both the H -field sensors and the sample covering coils, together with the compensation coils, to determine the J -value in the test sheet. The shape and arrangement of the coils were optimized by field modeling with the aim of limiting the variability of the H field in the required area to a value of $\pm 1\%$. Such instability in measurements for industrial purposes is entirely satisfactory.

The constructed system described in this article fulfills the requirements of sinusoidal output by a new adaptive algorithm.

The normative SST needs a specimen of 0.5×0.5 m. It is suited for spatial averaged parameters. To determine the local altered properties, the construction of the SST apparatus must be modified. In the presented solution, the specimen has the same dimensions as for the Epstein method. The field strength is measured with Hall sensors. To distinguish this method from the standard SST, we call it SST-H.

The authors of the article built the classic Epstein 250 apparatus and new SST-H design. Both are designed for the same dimensions of sheet samples, with the same powering and measurement system. The Epstein apparatus allows you to control the averaged parameters of the purchased sheets just like their manufacturers do.

The assumption of the SST-H design was to enable the control of changes in the magnetic properties of sheets under the influence of such activities that occur in the production process of an induction machine, i.e., squashing, bending, and drawing. It is known that such mechanical interactions deteriorate the magnetic properties of the sheets. To apply such influences in a controlled manner, a limited area is needed and sufficient, hence the limitation of the measurement area to about 50 mm comes from.

In the Appendix to this article there are some early results from testing the influence of bending on magnetic parameters. For now, there are too few to complete a separate article, but experiments show suitability of the discussed device.

2. Measurement hardware and methods

The entire measuring system consists of the following several elements:

- SST-H device,
- central measurement unit,
- amplifier,
- resistor,
- measurement-control computer.

The diagram of connecting individual elements is shown in Fig. 1.

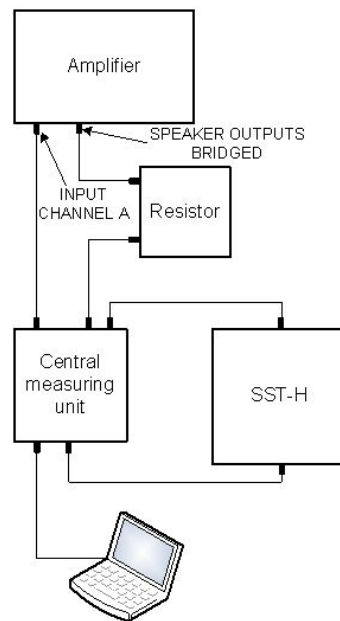


Fig. 1. Connection diagram for system components

The SST-H device is intended to test the properties of magnetic core sheets in the form of individual strips. Basically, it is provided for the same strips as for the Epstein device. In addition, it was also assumed that it would be possible to test individual, relatively small samples cut from sheets already subjected to technological operations when punching machine sheets. The actual measurement area covers a length of approximately 50 mm around the center of the sheet strip. For the normative SST system, significant differences in relation to the results of measurements with the Epstein apparatus at higher values of magnetic polarization were important. Annex B and C to EN 10280: 2001 + A1: 2007 (E) provide information tables and correction charts for the field strength H and loss p , as a function of the polarization value J , for adapting the measurement results with the SST apparatus to the results from the Epstein frame. For example, the percent correction values for the anisotropic sheet are given in Table 1.

Exponential extrapolation is recommended for higher polarization values.

The reason for these errors occurred was to determine the field strength H , as averaged from the value of the excitation current and the magnetic path. This methodically requires that the field strength value be constant along this path. The field strength value over the sample length can be calculated, inter alia, using the Finite Element Method (FEM), wherein the purpose of the determination is not the exact determination of the value of the field strength, but only the assessment of its variability. The calculations were made using the magnetostatic method, i.e. with the frequency of the exciting current equal to zero. Calculation results for the measurement system such as the one required in the standard indicate that the field strength is constant only in the central part of the sample. Figure 2 shows the distribution of the field image of H in the SST tester with a length of 300 mm with induction B in the saturation area.

Table 1. Correction values for anisotropic sheet (SST)

J [T]	dp [%]	dH [%]
1.0	1.7	6.1
1.1	1.8	6.3
1.2	2.1	6.6
1.3	2.4	7.4
1.4	2.8	9.0
1.5	3.3	12
1.6	4.0	17
1.7	5.0	27
1.8	6.0	43

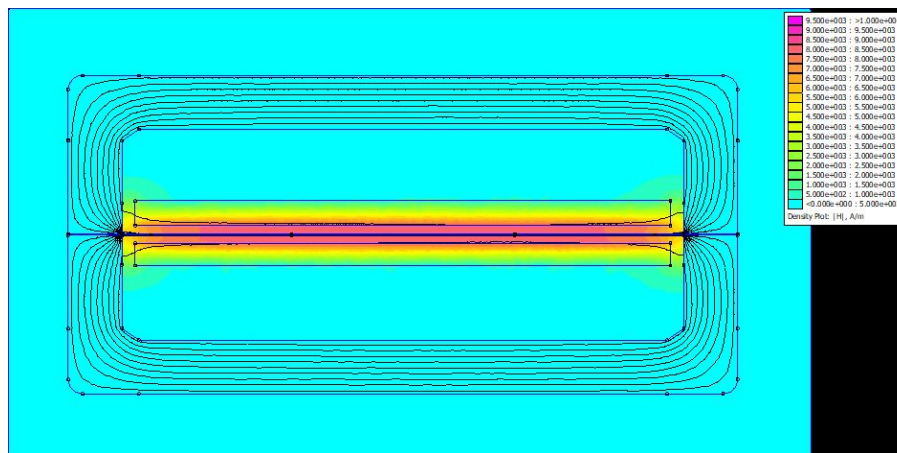


Fig. 2. Calculated distribution of the field strength H in SST along a 300 mm sample

The ampere-turns of the excitation windings were equal to 2 000, which would give an average H-field strength close to 8 000 A/m with the distance between the inner ends of the armature. It is higher in the middle of the sample and significantly lower at the ends. Therefore, the calculation of the field strength in the sample from ampere turns is not correct. Although in the vicinity of the sample center, the H values in this system are not very variable, but the direct measurement of H intensity using the hall effect sensor in this area is practically impossible due to lack of space.

The values of the longitudinal component of induction inside the sample in the area between the ends of the armature are also not constant, as shown in Fig. 3.

For this reason, the field strength value cannot be properly determined based on the excitation current measurement. Direct measurement of field strength in the middle of the sample using

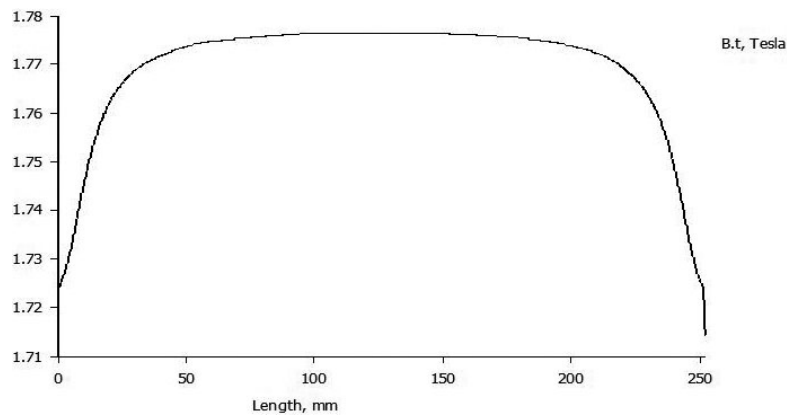


Fig. 3. Calculated distribution of flux density B in SST along a 300 mm sample

a continuous excitation coil like in a classic SST apparatus is not possible. Therefore, in the SST-H apparatus built by the authors, the field excitation system was changed in relation to the recommended standard. The modified excitation system consists of two separate coils in the Helmholtz layout. It provides a virtually constant field strength H value in a given space and lateral access to the field measurement. The outer magnetic circuit is made of electrical sheet. Figure 4 schematically shows the structure of the SST-H apparatus.

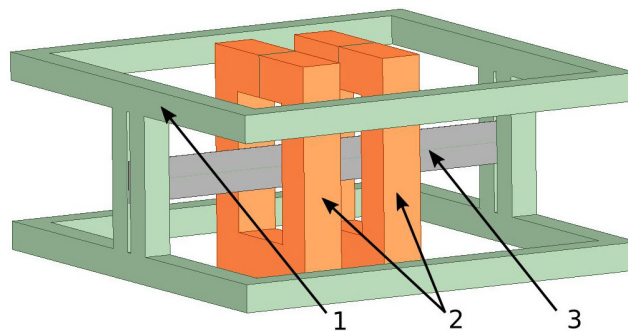


Fig. 4. Construction of the SST-H apparatus: 1 – outer magnetic circuit, 2 – excitation system in the Helmholtz layout, 3 – tested specimen

Simulations performed in the same way as for the classic SST design prove that the field strength is constant over a length of about 50 mm. The simulation results are presented in Figs. 5 and 6.

Hall effect sensors were used to directly measure the field strength. Two sensors, 50 mm apart, whose output voltages are added, were used to average the local field deviations caused by the heterogeneity of the material being tested.

The general view of the constructed SST-H apparatus is shown in Fig. 7.

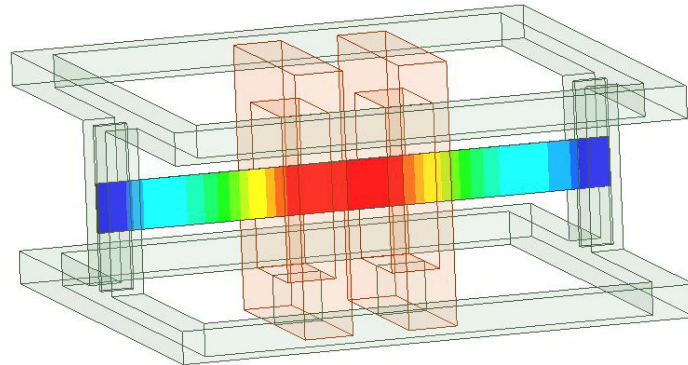


Fig. 5. Image of the magnetic field strength in the sample

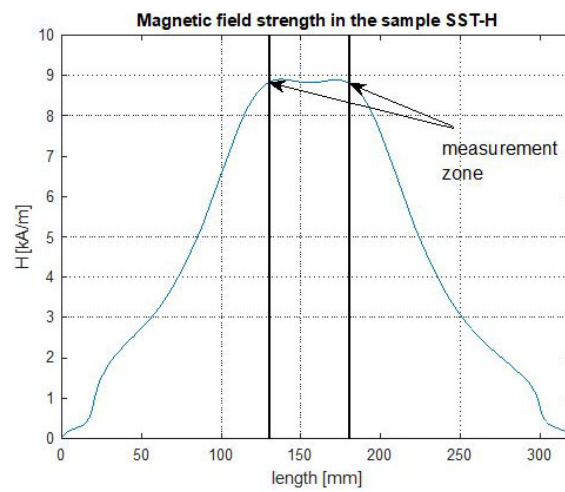


Fig. 6. Calculated distribution of field strength H in SST-H along a 320-mm sample

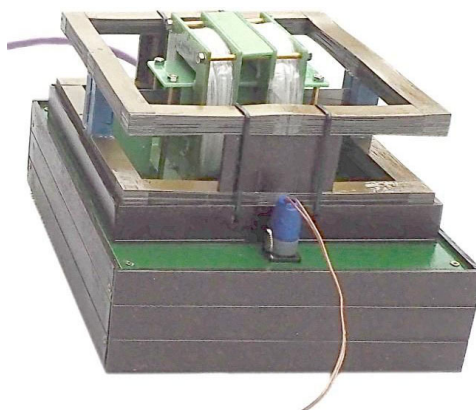


Fig. 7. Built SST-H measuring apparatus

In the constructed SST-H system, the maximum polarization values of J exceeded 1.9 T. This range is sufficient for designers of induction machines and significantly exceeds the loss values for $J = 1.5$ T given in the data sheet by manufacturer.

3. Waveform generation

Measurement standards [8] require sinusoidal waveforms of the induced voltage. The form factor of the voltage waveform cannot differ from the ideal sinusoidal by more than 1% (the ideal sinusoidal form factor is ~ 1.1107). It is not easy because of the nonlinear relationship between the magnetic field strength $[H]$ and the polarization $[J]$. This known relationship has also a hysteresis loop and will be different for each type of steel. Also, flux direction has a major influence on results even for material treated as isotropic. In paper [9] a quasi-Newton method is described, while the method presented in [10] involves Fast Fourier Transform (FFT) and adds inverted components of signals to the excitation signal. Both methods work for a limited range of polarization (not exceeding the saturation point). The method presented here was tested for J above 1.9 T, which was above the saturation point. The output hysteresis for the maximum value of J is shown in Fig. 8.

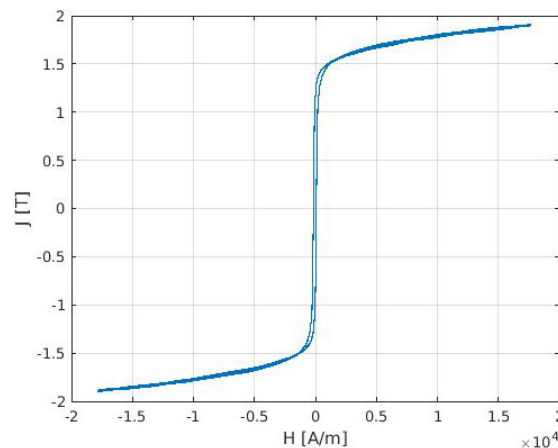


Fig. 8. Measured hysteresis loop for maximum value of J (1.9 [T])

4. Algorithm

The algorithm for obtaining sinusoidal voltage is quite simple:

- step 1: apply the sinusoidal waveform to the excitation coil (input),
- step 2: measure the voltage waveform from the measuring coil (measure the output),
- step 3: compare the output waveform with the desired waveform point by point and calculate the difference (1),
- step 4: modify each point of the input waveform, according to the difference calculated before and using the proportional coefficient (k),

- step 5: apply waveforms to the input,
- step 6: repeat steps 2–5 unless the output waveform is close enough to desired (2).

The presented algorithm works well up to about 1.5 T. To obtain a proper waveform in the whole range (0.2–2.0 T) it needs some modification. The main is that the proportional coefficient is not constant; it will be increased if there is no improvement during some number of iterations. The algorithm is used to get one characteristic point, for specific value of polarization. When the waveform for another point is calculated, the algorithm starts with the previous shape of the input voltage. It makes the calculation faster, especially for larger numbers of points in the range.

To calculate the difference of desired and output waveforms, we use:

$$err = \frac{1}{A} \cdot \sqrt{\frac{\sum_{n=1}^N (s_n - w_n)^2}{N}}, \quad (1)$$

where: N is the number of points in the whole period, s_n is the n -th point of an output waveform, w_n is the n -th point of a desired (normative) waveform, A is the amplitude of the waveform.

The root mean square value is calculated as usual:

$$RMS = \sqrt{\frac{\sum_{n=1}^N (s_n)^2}{N}}. \quad (2)$$

To obtain the form factor of the output waveform, we need to calculate the half-period average value:

$$We = \frac{1}{N} \sum_{n=1}^{N/2} |s_n|. \quad (3)$$

Then the form factor is calculated according to the formula:

$$FF = \frac{RMS}{We}. \quad (4)$$

Shapes of input waveforms during the iterations are shown in Fig. 9 and corresponding output voltage is shown in Fig. 10.

After 30 iterations, the shape is close to the sinusoidal. The exact form factor for iterations and corresponding difference from the sinusoidal form factor (1.1107) are presented in Table 2.

Table 2. Form factor (FF) during the iterations

No of iterations	FF	Difference (FF – 1.1107)/FF
10	1.15604	0.040821104
20	1.11726	0.005906185
30	1.10728	0.003079139

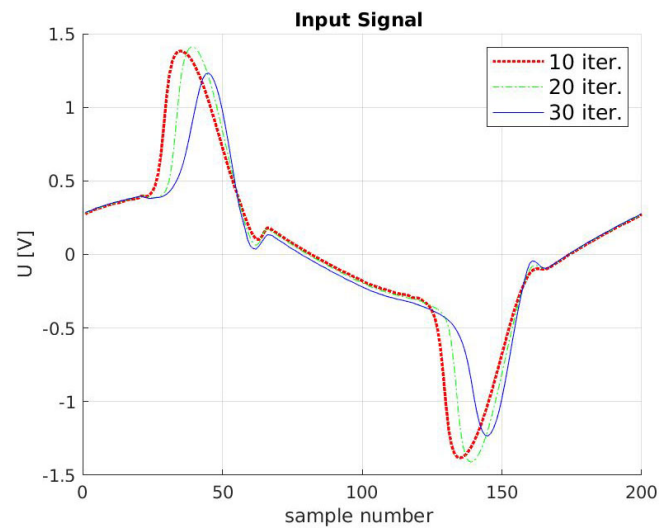


Fig. 9. The input waveform shapes during the iterations

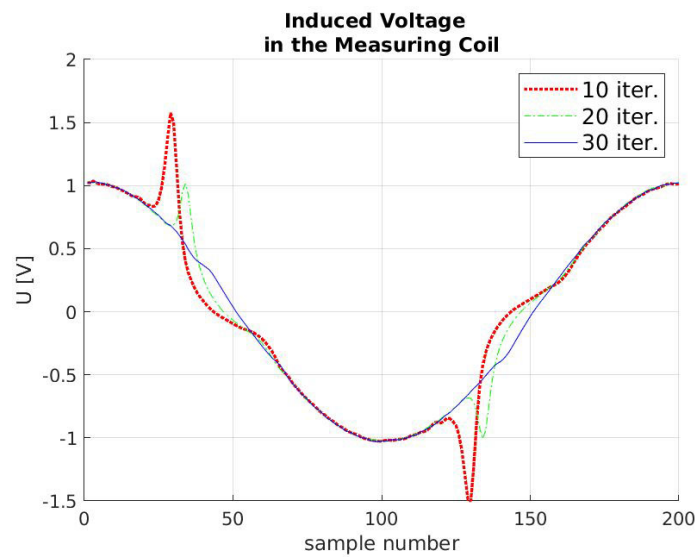


Fig. 10. Measured shape of the output voltage

The idea of variable coefficients in other applications is known [11, 12], here the main problem was to obtain proper ranges of change. Basically, the algorithm was tested in two ranges, the first one: small values of J (up to 1.0 T) and small numbers of iterations and the second one: high value of J (about 1.8 T) and higher numbers of iterations. The proper coefficient in these two cases was found, and this made the lower and upper value of the final coefficient.

5. Comparison of the results from the Epstein and SST-H apparatus

The samples cut along the (d) band and separately across the (q) band of the M400-50 E isotropic sheet, with dimensions adapted to the Epstein 250 apparatus, were first tested in the Epstein apparatus and then in the constructed SST-H. This allowed us to assess the relation of the SST-H results to those considered as basic from the Epstein apparatus. Since the J polarization values for specific measurement points from both apparatuses are always slightly different, the results were reduced to the same J values using quadratic local interpolation. Selected results, obtained at a frequency of 50 Hz, are presented in Figs. 11–16.

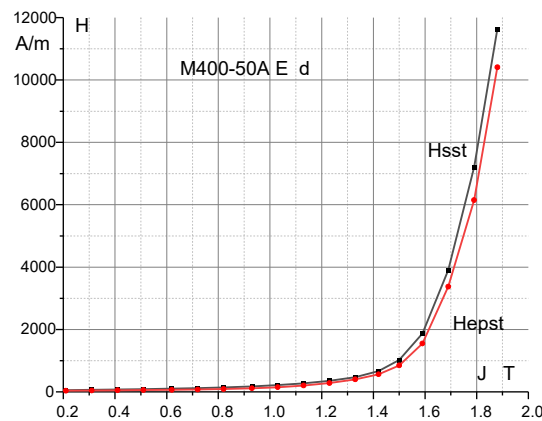


Fig. 11. H values depending on J for sheet M400-50 E – d

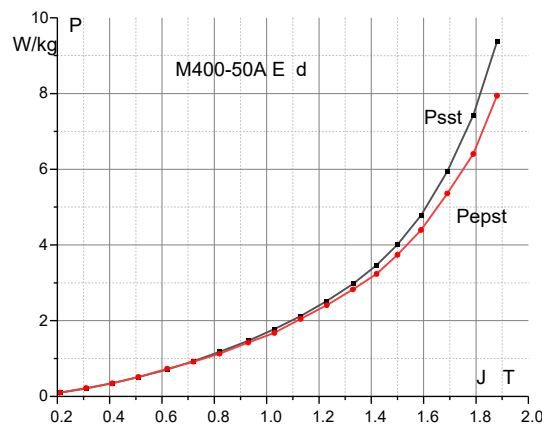


Fig. 12. Active loss as a function of J for sheet M400-50 E – d

The figures presented show that the values of H and, consequently, P up to the polarization value $J = 1.4$ practically coincide, both for the longitudinal and transversely cut samples. Above this value for the SST-H apparatus, they grow faster.

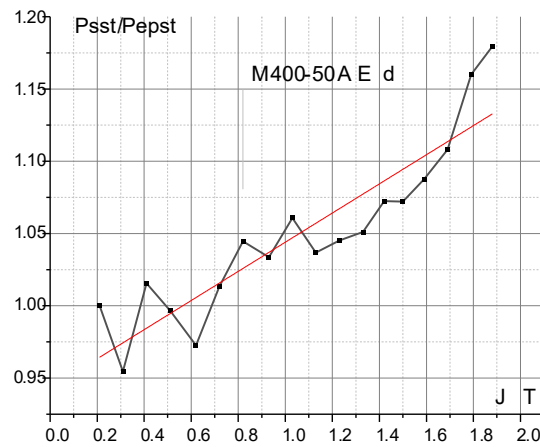


Fig. 13. Ratio of the loss values as a function of J of both apparatuses

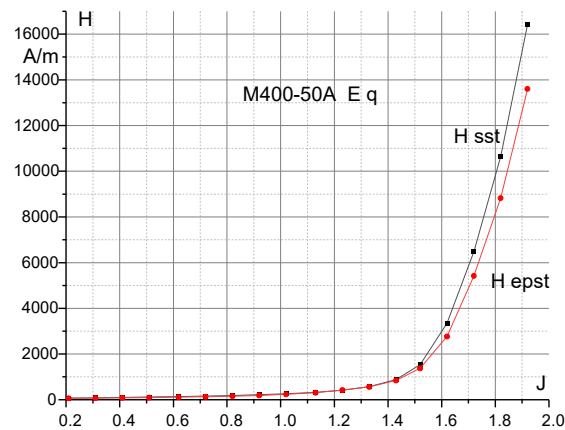


Fig. 14. H values depending on J for sheet E, cuted across band – q

The SST-H system for technically interesting polarization values gave P values close to those from the Epstein apparatus. However, it is known that in the Epstein apparatus the distribution of the H-field intensity is not constant for an induction above saturation. As a result of the measurements, average values of H, J, and P are obtained. Thus, these are not values that correspond to specific constant field values in the entire tested sample, as is assumed to be. The measurement method with the Epstein apparatus has been accepted as standard and correct [13]. In the range up to $J = 1.5$ T, for which sheet power losses are given by the manufacturers, the deviations are acceptable; however, for values close to 2 T they are significant.

The ratio of the loss values P changes with J, similarly to the recommendations of the EN 10280 standard. Formulating more general conclusions would require much more measurements of various types of sheet; further work on the SST-H apparatus will be continued.

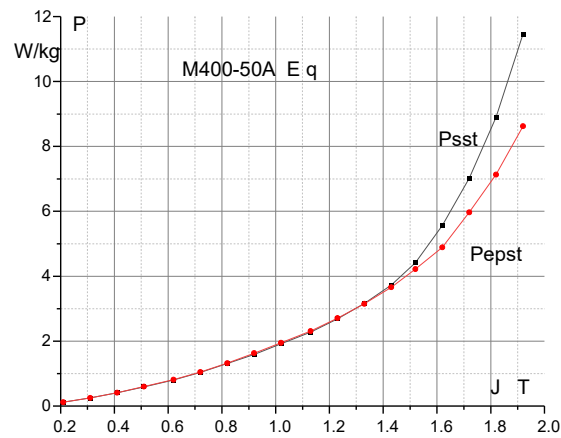


Fig. 15. Loss P values for E plate samples cut transversely

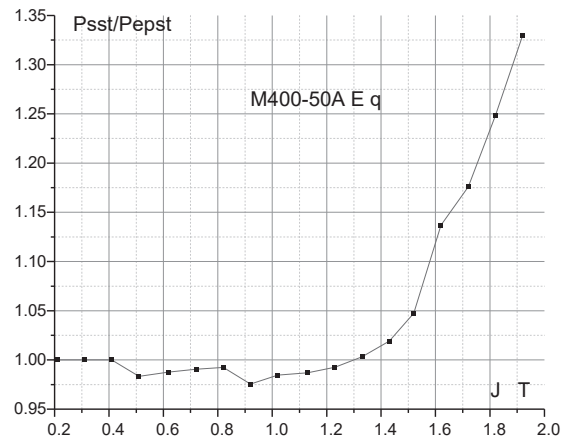


Fig. 16. The loss ratio obtained from two apparatuses for the E sheet – q

6. Summary

In the SST-H apparatus two important problems of this device have been significantly improved. Replacing the single distributed coil used in a standard SST apparatus, with two coils in the Helmholtz layout allows one to achieve approximately constant field strength, measured directly using the hall sensor. In this way, the measurement error is lower than in the standard SST apparatus and falls within the recommendations of the EN 10280 standard. Comparing the measurement results made with the Epstein apparatus with those made by the SST-H, the deviation of the measured values can still be seen. However, it can be suspected that due to the way it works, the measurements with the Epstein apparatus for induction values above 1.5 T are not correct.

The second, very important problem of matching the voltage curve for 1.5–1.9 T field density was solved thanks to the application of the adaptive control voltage generation algorithm. Thanks to this innovative method, the error of the induced voltage waveform form factor did not exceed 1%, for the entire measurement range, up to 1.9 T.

Appendix: The influence of sheet deformation

The constructed SST-H apparatus was used to test the magnetic parameters of sheet strips that were bent in the central part at different angles and then straightened. By measuring their characteristics, we investigated the influence of such deformation on the magnetic properties of the sheet. The measurement results are shown in Figs. 17 and 18. Experiments must be repeated under the controlled conditions, but the influence of such factors is clearly visible.

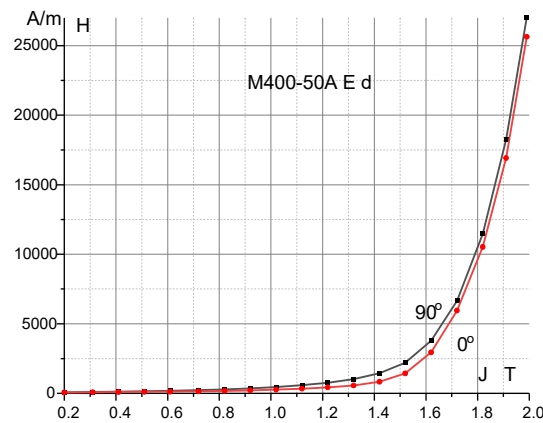


Fig. 17. The characteristics of $H(J)$ change with increasing bending angle for the E sheet – d

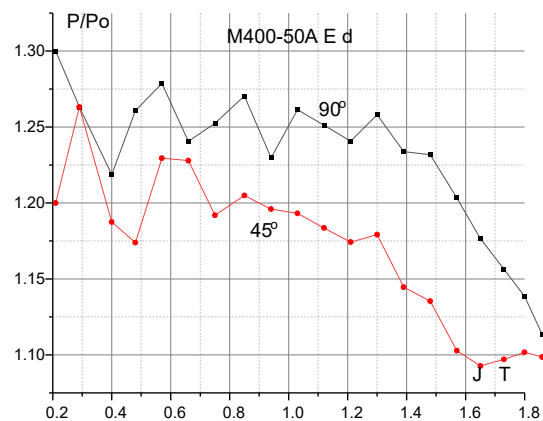


Fig. 18. Losses of the bent E sheet – d in relation to the original

References

- [1] Singh D., Rasilo P., Martin F., Belahcen A., Arkkio A., *Effect of Mechanical Stress on Excess Loss of Electrical Steel Sheets*, IEEE Transactions on Magnetics, vol. 51, no. 11, pp. 1–4 (2015), DOI: [10.1109/TMAG.2015.2449779](https://doi.org/10.1109/TMAG.2015.2449779).
- [2] Müller C., Elfgen S., Hameyer K., *Transient approach for iron loss separation of nongrain-oriented electrical steels considering the impact of cut edge effect*, Archives of Electrical Engineering, vol. 68, no. 2 pp. 237–244 (2019), DOI: [10.24425/aee.2019.128265](https://doi.org/10.24425/aee.2019.128265).
- [3] Xue S., Chu WQ., Zhu ZQ., Peng J., Guo S., Feng J., *Iron loss calculation considering temperature influence in non-oriented steel laminations*, IET Science, Measurement & Technology, vol. 10, no. 8, pp. 846–854 (2016), DOI: [10.1049/iet-smt.2016.0112](https://doi.org/10.1049/iet-smt.2016.0112).
- [4] Hofmann M., Kahraman D., Herzog H., Hoffmann M.J., *Numerical Determination of the Effective Magnetic Path Length of a Single-Sheet Tester*, IEEE Transactions on Magnetics vol. 50, no. 2, pp. 929–932 (2014), DOI: [10.1109/TMAG.2013.2283499](https://doi.org/10.1109/TMAG.2013.2283499).
- [5] Chen R., Zhang C., Li Y., Yang Q., Wang L., *An Improved Method for Measuring the Magnetic Properties of Silicon Steel with Double Sheets at High Frequency*, IEEE Transactions on Magnetics, vol. 55, no. 2, pp. 1–4 (2019), DOI: [10.1109/TMAG.2018.2868811](https://doi.org/10.1109/TMAG.2018.2868811).
- [6] Nakata T., Ishihara Y., Nakaji M., Todaka T., *Comparison between the H-coil method and the magnetizing current method for the single sheet tester*, Journal of Magnetism and Magnetic Materials, vol. 215–216, pp. 607–610 (2000), DOI: [10.1016/S0304-8853\(00\)00239-0](https://doi.org/10.1016/S0304-8853(00)00239-0).
- [7] Tumański S., Baranowski S., *Single strip tester with direct measurement of magnetic field strength*, Journal of Electrical Engineering-Elektrotechnicky Casopis, vol. 55, no. 10, pp. 41–44 (2005).
- [8] European standards EN 60404-2:1998, *Magnetic materials – Part 2: Methods of measurement of the magnetic properties of electrical steel strip and sheet by means of an Epstein frame*.
- [9] Yamamoto K., Hanba S., *Waveform control for magnetic testers using a quasi-Newton method*, Journal of Magnetism and Magnetic Materials, vol. 320, no. 20, pp. 539–541 (2008), DOI: [10.1016/j.jmmm.2008.04.015](https://doi.org/10.1016/j.jmmm.2008.04.015).
- [10] Chatziilias N., Meydan T., Porter C., *Real time digital waveform control for magnetic testers*, Journal of Magnetism and Magnetic Materials, vol. 254, pp. 104–107 (2003), DOI: [10.1016/S0304-8853\(02\)00761-8](https://doi.org/10.1016/S0304-8853(02)00761-8).
- [11] Peng X., Yao W., Yan C., Wen J., Cheng S., *Two-Stage Variable Proportion Coefficient Based Frequency Support of Grid-Connected DFIG-WTs*, IEEE Transactions on Power Systems, vol. 35, no. 2, pp. 962–974 (2020), DOI: [10.1109/TPWRS.2019.2943520](https://doi.org/10.1109/TPWRS.2019.2943520).
- [12] Ateş A., Alagöz B.B., Yeroğlu C., Alisoy H., *Sigmoid based PID controller implementation for rotor control*, European Control Conference (ECC), Linz, Austria, pp. 458–463 (2015).
- [13] Bavendiek G., Leuning N., Müller F., Schauerte B., Thul A., Hameyer K., *Magnetic anisotropy under arbitrary excitation in finite element models*, Archives of Electrical Engineering, vol. 68, no. 2, pp. 455–466 (2019), DOI: [10.24425/aee.2019.128280](https://doi.org/10.24425/aee.2019.128280).